

## Dynamics of Histone Acetylation in *Chlamydomonas reinhardtii*\*

(Received for publication, May 26, 1998, and in revised form, August 6, 1998)

Jakob H. Waterborg‡

From the Division of Cell Biology and Biophysics, School of Biological Sciences, University of Missouri, Kansas City, Missouri 64110-2499

**The dynamic character of core histone post-translational acetylation in the unicellular green alga *Chlamydomonas reinhardtii* was studied by tritiated acetate incorporation. Histone H3 is the major target of acetylation, steady state, and in pulse and pulse-chase analyses. Acetylation turnover rates were measured by tracer labeling under steady-state conditions. Half-lives of 1.5–3 min were found for penta- to mono-acetylation of H3, dynamically acetylated to the 30% level. Twenty percent of H3 was multi-acetylated, on average with 3.2 acetyl-lysines, all with rapid turnover. Deacetylase inhibitor trichostatin A (TSA) caused doubling of average acetylation levels, primarily as penta-acetylated H3, but half of H3 was not acetylated at all. The level of histone H4 acetylation was only half that of H3 and a major fraction of mono- and di-acetylated forms appeared static. The dynamic fraction had an average half-life of 3.5 min with higher turnover rates for more highly acetylated H4 forms. TSA, inhibiting less effectively deacetylases active on H4, strongly increased multi-acetylated H4 levels and doubled average acetylation. As for H3, half of histone H4 remained unacetylated. Acetylation of histone H2B was low and of H2A was barely measurable. Despite turnover with half-lives of approximately 2 min, no increase beyond di-acetylation was seen upon TSA treatment.**

The study of histone acetylation has its origin more than 30 years ago when Allfrey (1) established for the first time the correlation between high levels of histone acetylation and gene transcription. This was followed by the realization that histone acetylation is dynamic (2). In animal cells, histone acetylation has turnover half-lives of 3–30 min (3–7). Thus, locally highly acetylated chromatin on or near transcriptionally active or poised genes results from a localized shift in the dynamic equilibrium between histone acetyltransferase and deacetylase activities in favor of acetylation (8). In some cases, like *Saccharomyces cerevisiae*, the significant steady-state level of acetylation of H3 and H4 histones (9) is achieved under conditions of rather slow turnover with a half-life of 2 h (10). In recent years, histone H4 and H3, highly acetylated at some or all amino-terminal lysines, has been studied intensively by specific antibodies (11–14). This has confirmed the general relationship between high acetylation and gene transcription, although high acetylation at some sites is more clearly correlated with deposition of newly synthesized histone or even with gene or chromosome silencing (15).

\* This work was supported by a University of Missouri Research Board grant. The costs of publication of this article were defrayed in part by the payment of page charges. This article must therefore be hereby marked "advertisement" in accordance with 18 U.S.C. Section 1734 solely to indicate this fact.

‡ To whom correspondence should be addressed: Rm. 414 BSB, 5007 Rockhill Rd., Kansas City, MO 64110-2499. Tel.: 816-235-2591; Fax: 816-235-5158; E-mail: waterborg@cctr.umkc.edu.

The recognition that *n*-butyrate inhibited histone deacetylase *in vivo* and caused general and extensive hyperacetylation of chromatin led to experiments that in general supported correlation between high acetylation and gene transcription. It allowed measurements of acetylation turnover rates upon release of inhibition (5, 16). In recent years, many and more specific inhibitors of histone deacetylase have been discovered, including the reversible inhibitor trichostatin A (TSA)<sup>1</sup> and irreversible inhibitor trapoxin (17–19).

With the recent cloning of some histone acetyltransferases, starting with *Tetrahymena* (20), and the recognition that many transcription factors, co-activators, and basal transcription initiation complex proteins are, localize, or contain acetyltransferases in species from yeast to man, it has become apparent that multiple acetylating enzymes, each with potentially unique enzymatic substrate specificities and/or with unique localization mechanisms, act on chromatin at and away from the transcription initiation complex (15, 21, 22). Also, more and diverse histone deacetylase activities, and their localization adapters (23, 24), have been identified, from yeast to man and higher plants (22, 25–28). To date, all deacetylase activities described and tested can be inhibited *in vitro* by TSA, but with different efficiencies (29). In general, the correlation between acetylation and gene expression has been confirmed (22, 30–33) even while repression of some genes and functions has also become more clearly described (23, 29, 34).

Most studies of histone acetylation have been performed in animal cells, in fungi like *S. cerevisiae* or protists like *Tetrahymena*. In all these, histone H4 is the predominant target of histone acetylation, followed by histone H3, whereas acetylation of H2B and H2A core histones is lower. In higher plants, histone H3 is the predominant target of histone acetylation with rather high steady-state levels, especially of replacement variant forms which are preferentially localized in transcriptionally active chromatin domains (35–37). Acetylation levels of histone H4 are lower, and levels of H2B are lower still, whereas acetylation of histone H2A is barely detectable (38). In the unicellular green algae *Chlamydomonas reinhardtii*, this difference is even more pronounced, and steady-state levels of multi-acetylated H3 are remarkably high (39). Also, histone acetylation in *Chlamydomonas* appeared rather fast, as detected during analysis of histone synthesis throughout the cell cycle (39). This prompted study of the dynamics of histone acetylation. Described below is a unique quantitative analysis of the rate of turnover of acetylation with the highest rates of turnover for histone acetylation reported to date. It describes how fast and to which extent TSA induces hyperacetylation of histones, limited by histone methylation, and reports that a remarkably high fraction of the algal chromatin cannot be acetylated.

<sup>1</sup> The abbreviations used are: TSA, trichostatin A; AUT, acid/urea/Triton X-100; HPLC, high pressure liquid chromatography; HSM, high salt medium.

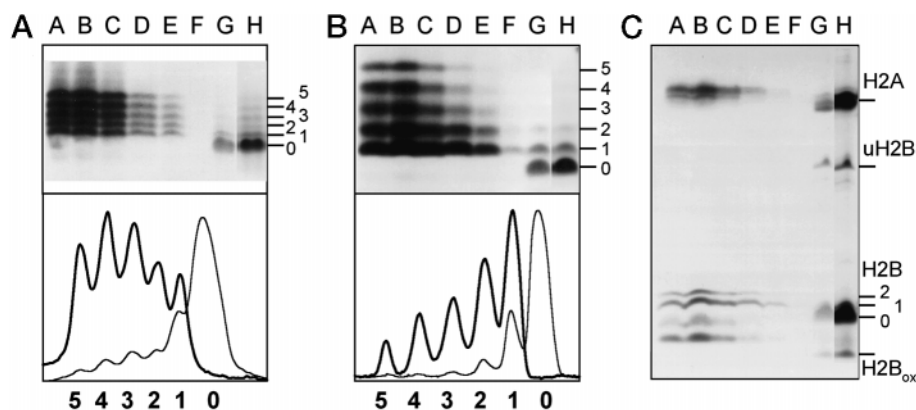


FIG. 1. AUT gel analysis of histones prepared from cells with and without cycloheximide. Comparison of tritiated acetate incorporation in histones of *Chlamydomonas* cells for 60 min without (G) or for 0 (A), 2 (B), 6.5 (C), 12 (D), 20 (E), or 60 min (F) with cycloheximide. A representative Coomassie-stained AUT gel lane (H) is shown for histone H3 (A), H4 (B), H2B and H2A (C). Fluorography was for 7 (A) or 21 days (B and C). As discussed in the text, the loss of radioactivity results from the turnover of radioactive acetyl groups with non-radioactive ones. Non-radioactive acetyl groups are of cellular origin, following exhaustion of the small pool of radioactive acetate supplied. At no time in this experiment was non-radioactive acetate added. The level of acetylation in each histone species is indicated by *small numerals* along the sides and along the bottom of Coomassie (*thin line*) and fluorograph (*thick line*) scans of histone H3 and H4 in the *bottom panels* of A and B, respectively. For histone H2B only the bands of the major form of H2B are marked. The presence of ubiquitinated H2B (uH2B) and oxidized H2B (H2B<sub>ox</sub>) is indicated. The existence of co-eluting and overlapping variant forms of H2A prevents band assignments and quantitative analysis (39).

#### EXPERIMENTAL PROCEDURES

**Culture of *C. reinhardtii***—Cell wall-deficient strain CC-400 *cw-15* mt+ clone DG-1 (39) was maintained on Sueoka's high salt medium (HSM) on 0.8% agarose at 25 °C and continuous light. Phototrophic culture at 28 °C, exposed to continuous white light at 75 microeinsteins photosynthetic active radiation (PAR) m<sup>-2</sup> and 3% CO<sub>2</sub>-enriched air bubbling, was inoculated directly from plates at an initial density of 10<sup>5</sup> cells/ml into HSM minimal medium in 800-ml glass cylinders (4 cm in diameter) (39). Typically, growing cultures at a density of 2–6 × 10<sup>6</sup> cells/ml were collected by centrifugation for 10 min at 7000 × *g* in 1-liter buckets at room temperature and were resuspended at a density of 5 × 10<sup>7</sup> cells/ml. Translation inhibitor cycloheximide was added to 10 μg/ml from fresh, non-sterile stock (2 mg/ml in 50% ethanol) 10 min prior to the addition of acetate. For labeling to steady state, 0.1 M NH<sub>4</sub>Ac was added to 0.2 mM final concentration 5 min prior to the addition of tritiated acetate. High specific activity [<sup>3</sup>H]NaAc (9 × 10<sup>13</sup> Bq/mol, NEN Life Science Products) was added at 3.7 × 10<sup>7</sup> Bq (1 mCi) per 40 ml of concentrated culture (to 10 μM acetate), and cells were incubated at room temperature for various lengths of time. Acetate incorporation was stopped by transfer to melting ice and collection of cells by centrifugation for 5 min at 650 × *g* and 0 °C. The chase condition in pulse-chase experiments was created by the addition of 1 volume of ammonium acetate-containing HSM (9.34 mM acetate) 2 min after tritiated acetate was added to 20 μM. Acetate labeling at reduced specific radioactivity was performed by addition of ammonium acetate to 200 μM followed after 5 min by the addition of tritiated acetate to 10 μM. Trichostatin A (Wako Bioproducts) was dissolved in dimethyl sulfoxide at 0.5 mg/ml (1.67 mM) and was used at a final concentration of 100 ng/ml unless otherwise indicated.

**Preparation and Analysis of Histones**—Isolation of nuclei and preparation of histones was essentially done as described previously (39). Briefly, histones from 2 × 10<sup>9</sup> cells were solubilized by sonication of the nuclear pellet in 40% guanidine HCl at pH 6.8, acidified, centrifuged, neutralized, bound to and eluted from 0.25 ml of Bio-Rex 70 resin (Bio-Rad) by 40% guanidine HCl, dialyzed extensively against 2.5% (v/v) acetic acid, and lyophilized. At all steps, 2-mercaptoethanol in excess of 1 mM was present. Histones were solubilized and subjected to reversed-phase HPLC on a Zorbax Protein-Plus column (4.6 × 25 mm) as described (39), developed by a 90-min gradient at 1 ml/min with acetonitrile between 30 and 60% (v/v) and 0.1% trifluoroacetic acid, and monitored by absorbance at 214 nm. Radioactivity in fractions was determined by liquid scintillation counting. Fractions were made 1 mM in 2-mercaptoethanol, pooled based on absorbance and/or radioactivity, and lyophilized. Histones were electrophoresed in 30-cm long discontinuous acid-urea-Triton (AUT) gels with 8 M urea and 9 mM Triton X-100, essentially as described (39, 40), until the methylene blue dye front had traversed one gel length (approximately 20 h at 300 V), except that histone H3 was run until methylene blue had traversed two gel lengths (approximately 44 h at 300 V). Procedures of AUT Coomassie gel staining, densitometry, and fluorography have been described pre-

viously (39). SigmaPlot version 4.0 (SSPS, Chicago) was used for non-linear regression data analysis.

#### RESULTS

**Pulse Labeling of Histones with Acetate**—Post-translational modification of the histones of unicellular green alga *C. reinhardtii* has been studied by incorporation of tritiated acetate into growing cells, synchronized by a light-dark regimen in acetate-free minimal medium during phototrophic growth (39). Labeled acetate is rapidly metabolized and incorporated into newly synthesized protein, which is observed as label incorporation into all histone species, separated by reversed-phase HPLC, after labeling for 60 min. Reducing the time of labeling to 5 min abolished most but not all label incorporation into non-acetylated histone forms (39) (results not shown). Preincubation of cells with translation inhibitor cycloheximide (10 μg/ml) completely abolished acetate incorporation into the co-translationally, amino-terminally acetylated linker histone H1 species and into the many low abundance proteins observed during HPLC fractionation of the crude histone preparation. Acid-urea-Triton (AUT) gel analysis and fluorography (Fig. 1) confirmed these observations and the absence of any acetate label incorporation into non-acetylated core histones, including histone H4 and H2A, histones that are typically co-translationally acetylated at the amino termini of newly synthesized polypeptides. Provided cycloheximide was added at least 5 min prior to the addition of tritiated acetate, (co)translational labeling of histones by acetate was prevented for more than 2 h.

The relative levels of post-translational incorporation of acetate into core histones following a short incubation with tritiated acetate differed markedly between histone species (Table I) and correlated well with steady-state acetylation levels of each histone, determined by Coomassie staining and densitometry of AUT gels (39) (compare lanes G and H in Fig. 1). Whereas in animal cells histone acetylation is highest in histone H4 and significant for all other core histones, in *Chlamydomonas*, even more than in higher plants (35–38), histone acetylation of H3 is predominant, acetylation of H4 is lower but significant, and acetylation of H2B and H2A is low, especially when judged by the relative post-translational incorporation of radioactive acetate (Table I).

**Instability of Lysine Acetylation Measured by Pulse and Pulse-Chase Experiments**—Turnover rates of dynamic, post-

TABLE I  
Histone comparison by steady-state acetylation levels and post-translational acetate labeling

Histone	HPLC labeling <sup>a</sup>	AUT gel: labeling <sup>a</sup>	Coomassie densitometry		Fluorograph densitometry	
			MultiAc <sup>b</sup>	AcLys/H <sup>c</sup>	*MultiAc <sup>b</sup>	*AcLys/H <sup>c</sup>
H3	≡1.0	≡1.0	24 ± 1% (n = 6)	0.92 ± 0.05 (n = 6)	83 ± 1% (n = 5)	2.94 ± 0.17 (n = 8)
H4	0.39	0.52	10.0 ± 0.4% (n = 7)	0.47 ± 0.01 (n = 6)	66% (29%)	2.25 (1.6 ± 0.1 (n = 5))
H2B	0.15	0.08	3.3 ± 0.3% (n = 7)	0.18 ± 0.01 (n = 7)	36% (14%)	1.38 ± 0.03 (n = 3) (1.15 ± 0.08 (n = 3))
H2A	0.14	0.03	— <sup>d</sup>	—	— <sup>d</sup>	—

<sup>a</sup> Cells were incubated with tritiated acetate as shown in Fig. 2. The specific radioactivity "labeling" of histones was measured as cpm per absorbance at 214 nm during HPLC fractionation (39) and by densitometry of Coomassie-stained and fluorographed AUT gels (Fig. 1). Values were standardized on histone H3 which incorporated approximately 50,000 cpm per nmol of histone H3 when  $1.8 \times 10^9$  cells were incubated for 2 min with 1 mCi of tritiated acetate.

<sup>b</sup> Densitometry of Coomassie-stained AUT gels yields the percentage of histone existing in each acetylated form and the fraction of histone with more than 1 acetylated lysine per molecule (multiAc). Constant values are given as average with standard deviation and number of independent samples (n). Densitometry of fluorographs yields the same data, for those histones labeled by tritiated acetate (\*multiAc). The values obtained after 2 min and, within parentheses, after 60 min are given when levels decreased.

<sup>c</sup> The level of lysine acetylation of each histone species can be expressed as the average number of acetylated lysines per unlabeled (AcLys/H) and per labeled histone molecule (\*AcLys/H), taking into account the number of acetylated lysines in each form (39). It facilitates comparison of acetylation levels among histone forms that differ in distribution patterns (Fig. 1).

<sup>d</sup> AUT gel overlap of variant H2A forms prevents quantitation.

translational acetylation of histones are high with reported half-lives measured by pulse-chase experiments ranging from 3 min in mammalian cells in culture for the fastest dynamic component (4) to 2 h for the rather stable acetylation of H4 in *S. cerevisiae* (10). Less quantitative analyses provide rough estimates of half-lives of 10 or 20 min for higher plants (38). *Chlamydomonas* grown phototrophically, free of a carbon source other than CO<sub>2</sub>, appeared to be well suited to perform pulse-chase experiments. Very rapid incorporation of radioactive acetate, applied at a concentration of 10 μM, was followed by apparent rapid exhaustion of the small labeled acetyl-CoA pool, as judged by the pattern of acetate incorporation into individual histones (Fig. 2) and into acetylated forms of these histones (Fig. 1). Incorporation of acetate into cells upon addition of tritiated acetate, immediately followed by collection of cells and lysis as the start of preparing nuclei, typically gave label incorporation between 50 and 80% of the maximum value reached after incubation for 2 or 3 min. Between 2 and 20 min, apparent exponential decay of the specific radioactivity in each core histone species was observed with a half-life of  $6 \pm 1$  min (Fig. 2). This value should be considered an upper limit for the turnover rate because no real chase, *i.e.* dilution of the acetate pool, was applied.

The relative rate of acetyl-lysine turnover of a histone species at each level of modification can be determined from the change in specific radioactivity of each modification level by densitometry of Coomassie-stained and -fluorographed AUT gels. The pattern observed for histone H3, acetylated at 5 sites (Fig. 1A), is clearly different from that of histone H4 (Fig. 1B), despite the fact that H4 is also acetylated at 5 lysines. The rate of acetyl-lysine turnover is essentially identical for each level of modification of H3 (Fig. 3) yielding a pattern that is fading over time as radioactively labeled acetyl-lysines are turned into non-radioactive ones, without a change in distribution (Fig. 1A). In contrast, it is clear from the much more rapid fading of the multi-acetylated bands in the histone H4 pattern (Fig. 1B) that turnover is faster for penta- and tetra-acetylated forms than for di- or mono-acetylated species (Fig. 3B). This does not imply that highly acetylated forms of H4 lose acetyl groups and are converted into less and less modified forms because the steady-state pattern of H4 acetylation, measured from the Coomassie Blue distribution in AUT gels, does not change over time. The labeled acetylation pattern of histone H2B, with most label in mono- and di-acetylated forms, showed a slight shift over time (Fig. 1C) and a slight tendency for a higher turnover rate for higher modified forms (Fig. 3C). A similar

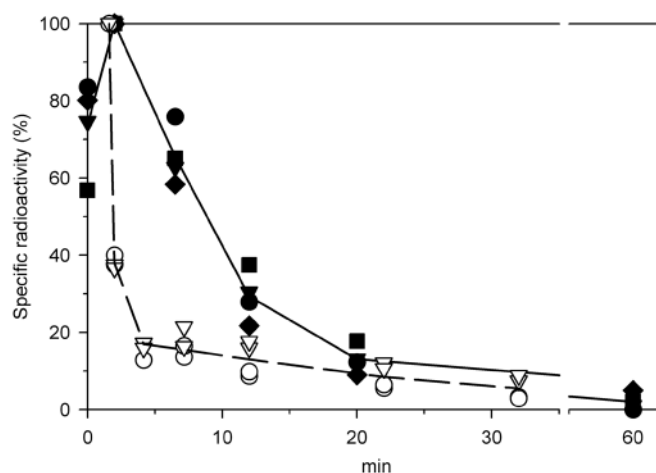
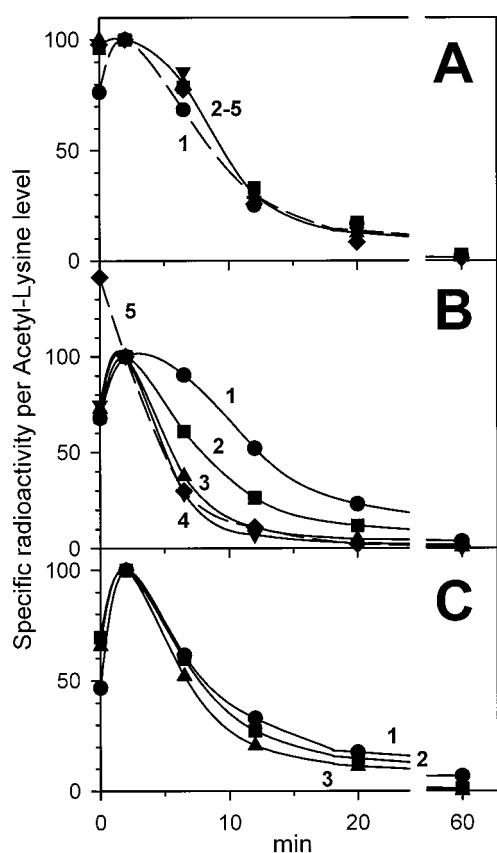


FIG. 2. **Dynamic changes in radioactive acetate labeling under pulse and pulse-chase conditions.** The relative specific radioactivity of histone H3 (circles), H4 (triangles), H2B (squares), and H2A (diamonds) was determined by densitometry of Coomassie-stained and fluorographed AUT gels and was standardized, setting the specific radioactivity at 2 min (Table I) to 100%. Similar values, obtained from HPLC analysis, are not shown. *Solid symbols* represent results obtained when tritiated acetate was added to cell cultures, and cells were collected and processed after the time shown along the bottom axis. *Open symbols* represent a pulse-chase experiment where 1 volume of growth medium with 9.34 mM ammonium acetate was added 2 min after the addition of tritiated acetate (10 μM). These values were standardized on the specific activity obtained after 2 min.

result was deduced for histone H2A, but the overlapping pattern of two variant protein forms (39) prevents quantitative analysis.

A pulse-chase protocol was used to measure turnover rates of histone acetylation. A 450-fold excess of unlabeled acetate was added 2 min after addition of tritiated acetate to cultures, pre-treated with cycloheximide. Histones were prepared, and their specific radioactivity was determined during HPLC fractionation (results not shown) and by densitometric analysis of stained and fluorographed AUT gels (Fig. 2). The instantaneous sharp drop in labeling of all histone species clearly demonstrated that the acetyl-CoA pool in *Chlamydomonas*, growing phototrophically, is very small. It also showed that acetylation turnover is very fast, faster than can be measured with reasonable accuracy by the experimental method used. Although cooled quickly at the end of each incubation, cells must be collected by centrifugation before they can be lysed in the



**FIG. 3. Comparison of relative rates of acetyl-lysine turnover during acetate pulse labeling.** The relative specific radioactivity of histone H3 (A), H4 (B), and H2B (C), obtained in the experiment of Fig. 2 when no non-radioactive acetate was added, was plotted per level of histone acetylation, relative to the specific activity of each form achieved after 2 min labeling with tritiated acetate in the presence of cycloheximide. Acetylation levels between 1 and 5 are marked by circles, squares, triangles, inverted triangles, and diamond symbols, respectively, and by numbers along the data. A single line in A represents all data, except for mono-acetylated H3 which is marked by a broken line. Penta-acetylated H4 in B is shown by a broken line.

procedure to prepare nuclei and histones. During this time, acetylation incorporation and turnover will occur, as judged by loss of acetate incorporation after "0"-min chase (Fig. 2).

**Turnover rates of Acetyl-lysines by Labeling to Steady State**—One can measure rates of turnover from the pattern of specific radioactivity if conditions are used that allow labeling under steady-state conditions. An apparent steady-state condition of the acetyl-CoA pool in phototrophically growing *Chlamydomonas* cells could be achieved for a period of 1 h by the addition of a single dose of ammonium acetate to a final concentration of 200  $\mu\text{M}$ . This was experimentally established by determining whether labeling to a constant specific radioactivity of histone H3 and H4 in HPLC elution profiles could be achieved, lasting for at least 1 h, when 10  $\mu\text{M}$  tritiated acetate was added between 5 and 30 min after addition of ammonium acetate to 50, 100, 200, 400, and 800  $\mu\text{M}$  to cycloheximide-treated cultures. Ammonium acetate at 200  $\mu\text{M}$  represented the optimal choice of an apparently stable acetyl-CoA pool into which the tritiated acetate could be added as tracer, without excessively reducing the specific radioactivity of the pool and of acetylated histones. Fig. 4 gives a representative example of the rise in specific radioactivity measured during reversed-phase chromatography and by densitometric analysis of stained and fluorographed gels. SDS gel analysis at several gel loading levels was combined with different fluorography exposures to ensure that specific activities were determined within linear ranges of Co-

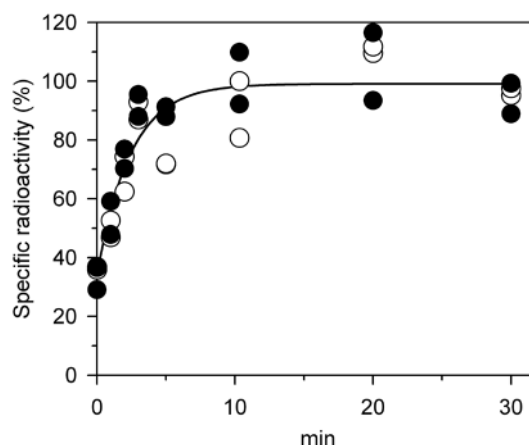


**FIG. 4. Radioactive acetylation of histone H2B under steady-state acetyl-CoA pool conditions.** The specific radioactivity pattern of histone H2B is shown as a representative example of specific radioactivity measurements made in HPLC fractions (open symbols) and by densitometry of Coomassie-stained and fluorographed gel lanes (solid symbols) when 10  $\mu\text{M}$  tritiated acetate is added to a culture of *Chlamydomonas* cells, preincubated for 15 min at 10  $\mu\text{g/ml}$  cycloheximide and for 5 min at 200  $\mu\text{M}$  ammonium acetate in minimum medium and phototrophic growth conditions. The data were fitted to a nonlinear regression pattern of exponential rise to a maximum (shown as 100%), and the fitted curve is shown. The standard error in this example was calculated as 17% for the slope and 10% for the maximum.

massie staining and film darkening. AUT gel analysis of histone H3 and H4 was used to determine the pattern of specific radioactivity over time for each acetylated form. The data were fitted by nonlinear regression to a pattern of an exponential rise to a maximum value, and single component fits were obtained for all data. Half-life values calculated were  $1.4 \pm 0.3$  min for H2B (Fig. 4),  $2 \pm 1$  min for H2A,  $3.5 \pm 1.1$  min for H4, and  $1.7 \pm 0.2$  min for four independent measurements of total histone H3. Table II lists half-life values calculated for each of the acetylation levels of histone H3. As expected from the pulse label experiments (Figs. 1A and 3A), the rates of turnover at each level of histone H3 acetylation were very similar. Although not significantly different, consistent with the relative rates of turnover during pulse label experiments (Fig. 3A), comparison across the acetylated forms suggests that highly acetylated forms of H3 may be deacetylated somewhat faster than less modified forms (Table II), a weak reflection of the same trend observed for histone H4 (Fig. 3B). Due to the limited accuracy in measuring the amounts of multi-acetylated histone H4 forms in Coomassie-stained AUT gels (Fig. 1B), reproducible half-life values for individual acetylated forms of histone H4 could not be calculated.

Labeling to steady state allows one to assess to which degree steady-state patterns of histone acetylation are dynamic or excluded from turnover. Data fit analysis to any experimental data set that converged properly (Fig. 4) showed the presence of only a single rate component for acetyl-lysine turnover. The specific radioactivity levels attained for histone H3 was analyzed for each of the five acetyl-lysine levels from stained and fluorographed AUT gels (not shown). It was standardized to the overall level of histone acetylation, on average 0.75 acetyl-lysine groups per histone H3 molecule (Table II). In case every acetyl-lysine is deacetylated and subsequently acetylated to the specific radioactivity of the acetyl-CoA pool, this standardization will yield specific radioactivity values identical to the number of acetyl-lysines per histone molecule. Within experimental accuracy, this was observed for histone H3 (Table II). The somewhat low value for penta-acetylated H3 may reflect that not every penta-acetylated H3 is subject to turnover or, more likely, that one of the five acetyl-lysines is less accessible.

TABLE II  
Quantitative analysis of histone H3 and H4 acetylation steady-state labeling and turnover

Ac-Lys level	Histone H3				Histone H4		
	Steady-state level <sup>a</sup>	Half-life	Standard specific radioactivity <sup>b</sup>	Dynamic fraction <sup>c</sup>	Steady-state level	Standard specific radioactivity	Dynamic fraction
		<i>min</i>		<i>%</i>			<i>%</i>
0	68.2 ± 0.8%	NA <sup>d</sup>	NA	NA	67.2 ± 1.9%	NA	NA
1	11.5 ± 0.7%	2.8 ± 0.8	1.1 ± 0.2	110 ± 17	22.7 ± 0.8%	0.7 ± 0.1	39 ± 16
2	7.2 ± 0.4%	1.8 ± 0.3	1.8 ± 0.2	92 ± 9	6.6 ± 0.4%	2.1 ± 0.3	58 ± 8
3	6.1 ± 0.4%	1.8 ± 0.7	3.1 ± 0.6	104 ± 20	2.1 ± 0.4%	4.4 ± 0.4	81 ± 7
4	4.2 ± 0.3%	1.6 ± 0.3	4.2 ± 0.4	106 ± 10	0.8 ± 0.3%	7.2 ± 1.0	≡100 ± 15
5	2.8 ± 0.2%	1.5 ± 0.4	4.1 ± 0.7	82 ± 15	0.6 ± 0.2%	6.8 ± 1.2	76 ± 13
All	0.75 ± 0.02	1.9 ± 0.4	0.75 ± 0.09	≡100 ± 12	0.48 ± 0.04	0.48 ± 0.04	55 ± 4

<sup>a</sup> The steady-state acetylation level, determined by densitometry of Coomassie-stained AUT gels, is given as relative values for each of the acetylation levels and for total histone as the average number of acetyl-lysines per histone molecule. Standard deviation errors are given for histone H3 ( $n = 8$ ) and H4 ( $n = 4$ ). All other errors shown are standard errors, calculated by the nonlinear regression fit of data to an exponential rise-to-max curve.

<sup>b</sup> The steady-state specific radioactivity was determined from AUT gel densitometry and numerically standardized on the average number of acetylated lysines per histone molecule. This standardization implies that the values will be identical to the numerical level of lysine acetylation in case every acetyl-lysine moiety, or a constant fraction of all modified lysines at each level, is turning over and has reached the specific radioactivity of the steady-state acetyl-CoA pool.

<sup>c</sup> The maximum dynamic fraction of each acetylated form was calculated based on the condition that the value of the standardized specific radioactivity cannot exceed the number of acetyl-lysines for any level. The ≡ sign indicates the assumption made. For histone H4, the minimum condition is only reached when all acetyl-lysines in tetra-acetylated H4 are turning over and have reached the specific radioactivity of the steady-state acetyl-CoA pool. However, if not all these sites are dynamic, the dynamic fraction of acetyl-lysines in the other acetylated forms will decrease proportionally. The dynamic fraction calculated for all of H3 and H4 is obviously limited to those histone molecules that contain at least one acetylated lysine.

<sup>d</sup> NA, not applicable.

Overall, the close correlation between specific radioactivity levels and level of acetylation suggests that all acetylated histone H3 molecules, at every available amino-terminal lysine (9, 14, 18, 23, and 27 (39)), are continuously deacetylated and re-acetylated with a half-life of approximately 2 min (Table II).

The same analysis applied to histone H4 yields completely different results. Although the absolute level of acetylated H3 and H4 molecules in *Chlamydomonas* is comparable, the distribution over mono- through penta-acetylated forms is not (Table II). Based on the relative labeling levels, at most all of tetra-acetylated H4 could be subject to dynamic acetylation at all sites. In this case, at least 40% of the acetyl-lysine groups in di- and 60% in mono-acetylated H4 are stable (Table II). Consequently, maximally 16% of histone H4 with an average level of 1.6 acetyl-lysines per molecule can be involved in dynamic acetylation in *Chlamydomonas* relative to maximally 32% for histone H3 with, on average, 2.4 acetyl-lysines. A previous estimate, based on different experimental analyses, noted that 19% of total histone H3, multi-acetylated with an average level of 3.2 acetylated lysines, might be involved in dynamic acetylation (39). Limited to multi-acetylated forms as before, the current study concludes that maximally 20.3% of histone H3 is dynamic and multi-acetylated with, on average, 3.2 acetylated lysines. The absolute specific radioactivity of histones H3 and H4 was calculated as cpm per absorbance in reversed-phase chromatography fractions following steady-state labeling. Setting the observed specific radioactivity of histone H3 to 100%, histone H4 was labeled at the  $57 \pm 9\%$  level. This level is higher than after a 2-min pulse label (Table I), consistent with a slower rate of turnover (see above). As far as can be concluded from these necessarily rough calculations, it appears likely that at least a major fraction if not all of tetra-acetylated H4 at all sites is subject to acetyl turnover and thus that close to 15% of histone H4 is involved in dynamic acetylation.

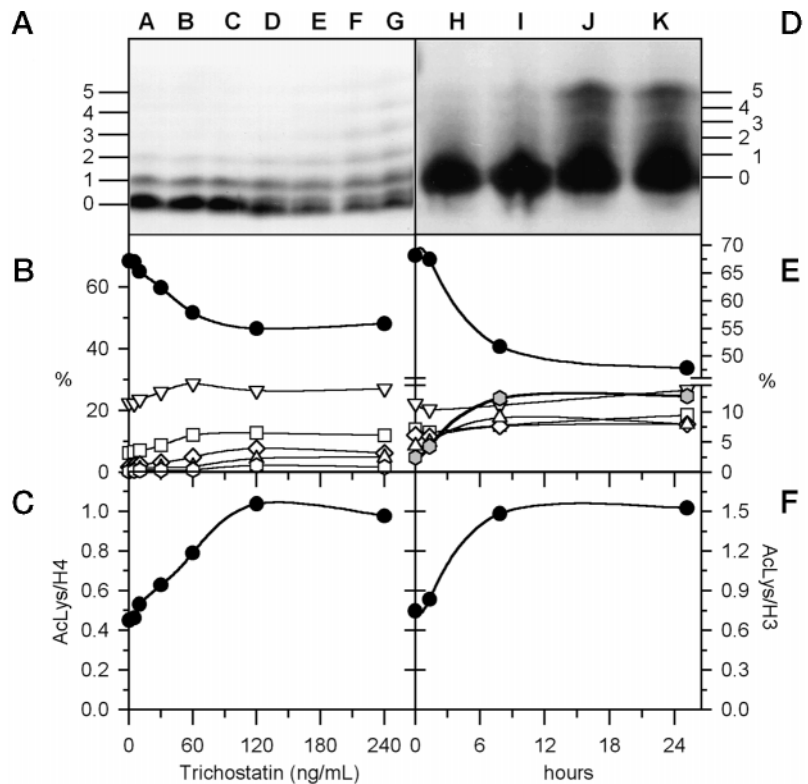
*Induction of Histone Hyperacetylation by TSA*—TSA has been shown to act as a potent reversible inhibitor of histone deacetylases, effective at micromolar concentrations (17). Treatment *in vivo* leads rapidly to extensive hyperacetylation of core histones. TSA has been used in *Phaseolus* (beans), and chromosome acetylation levels were affected, as detected by acetyl-lysine-specific antibodies (41). To date, concentration

and time dependence of TSA effects in plants and the extent of induced hyperacetylation have not been studied.

A range of concentrations of TSA was applied to *Chlamydomonas* culture for 1 h to determine an effective concentration. Measured as increasing levels of histone acetylation, *e.g.* of histone H4 (Fig. 5A), steady-state acetylation increased detectably even at the lowest concentrations tested (5 ng/ml). It reached stable levels at a concentration of 100 ng/ml (0.33  $\mu$ M) (Fig. 5C) after doubling the level of H4 acetylation (Fig. 5C) by increasing the abundance of each multi-acetylated form, at the expense of a 20% drop in unmodified histone H4 (Fig. 5B). Similar hyperacetylation was observed for histone H4 and H3 when *Chlamydomonas* cells were cultured phototrophically for up to 25 h at 100 ng/ml TSA (Fig. 5F). In both experiments, the pattern of H3 hyperacetylation was qualitatively different from that of H4. The rise in H3 acetylation was almost completely due to increases in the amount of the penta-acetylated histone form (Fig. 5E), the highest discrete level of modification seen for H3 (Fig. 5D). Under neither condition were any changes detected in the low levels of charge-modified forms of H2B and H2A (results not shown).

Histone deacetylase inhibitors like butyrate or TSA induce hyperacetylation of histone H4 in animal cells until the non-acetylated form becomes a minor component and highly acetylated, tri-, and tetra-acetylated forms accumulate. Tetra-acetylated H4 is the maximally acetylated form in animals because lysine 20 in animal H4 is quantitatively methylated, which, as an irreversible modification, prevents acetylation (2). In *Chlamydomonas*, maximally acetylated histone H4 does not accumulate upon incubation with TSA (Fig. 5B). Penta-acetylated H4 is the highest level of acetylated histone H4 detected (Fig. 1B). Based on the deduced primary protein sequence (42, 43) and the fact that histone H4 in all plants analyzed is unmethylated (44), apparently all amino-terminal lysines at positions 5, 8, 12, 16, and 20 can be acetylated in *Chlamydomonas*. In contrast to H4, histone H3 does accumulate its maximally acetylated form, penta-acetylated H3 (Figs. 5E and 6G), which has been shown to undergo acetylation at lysines 9, 14, 18, 23, and 27, due to virtually complete methylation of lysine 4 (39). The detectable rise in tetra-acetylated H3 (Figs. 5E and 6G) may also represent a completely modified histone

**FIG. 5. TSA affects histone acetylation levels.** *Chlamydomonas* cells were incubated for 1 h in the presence of cycloheximide with TSA between 0 and 240 ng/ml (lanes A–G). **A** shows the Coomassie staining pattern of histone H4 after AUT gel analysis. **D** shows the acetylation pattern of histone H3 in a Coomassie-stained AUT gel following phototrophic growth of *Chlamydomonas* cells without (lane H) and with 100 ng/ml TSA for 80 min (lane I), 8 h (lane J), and 25 h (lane K). Acetylation levels are marked along the side of these panels. **B** and **E** show gel quantitation of all acetylated species of H4 and H3, respectively. Symbols used for 0, 1, 2, 3, 4, and 5 acetyl-lysines per histones are circles, inverted triangles, squares, diamonds, triangles, and hexagons, respectively. The curves for non-acetylated histone are shown in **bold** with **solid** symbols. Penta-acetylated histone H3 in **E** is emphasized by gray symbols. **C** and **F** show the average number of acetyl-lysine groups in H4 and H3, respectively.



H3 molecule since it is known that 1 in 4 lysine residues at position 27 are methylated (39). However, even for histone H3, the steady-state level of histone acetylation induced by TSA remains limited (Fig. 5).

The failure to induce extensive hyperacetylation in *Chlamydomonas* could result from an inherent difference between animals and algae or plants. Preliminary experiments in alfalfa have studied histone hyperacetylation in response to TSA. (i) The two histone H3 variants accumulate increasing levels of maximally acetylated H3. (ii) Histone H4 and H2B acetylation levels increase without reaching maximal acetylation status. (iii) The average level of histone acetylation only increased by 50–100%. To date, more distinct histone deacetylase activities have been described for plants than animals (25–28), and their sensitivity to inhibitors like TSA has not been established in every case. It may be that partial or selective inhibition of algal deacetylases establishes a new balance between histone acetylation and de-acetylation when TSA is added to cultures of *Chlamydomonas*.

The following experiment was designed to evaluate this hypothesis. *Chlamydomonas* cells in cycloheximide were incubated for increasing lengths of time with TSA. During the last 3 min, tritiated acetate was added to achieve maximum label incorporation (Fig. 2) in order to demonstrate to which extent dynamic histone acetylation was inhibited, either due to the direct inhibition of histone deacetylase activity or due to the resulting absence of potential acetylation substrate sites. Fig. 6 presents some of the results observed for histone H4 (Fig. 6, A–D) and H3 (Fig. 6, E–H). During incubation of cells with TSA for up to 1.5 h, histone H4 shows increasing levels of multi-acetylated forms (Fig. 6A), whereas histone H3 shows increasing levels of penta-acetylated histone (Fig. 6E). The quantitation of these changes (Fig. 6, C and G) gives patterns similar to those reported above (Fig. 5, B and E).

During this experiment, distinct phases can be identified, based on the results of the acetate tracer study. In the first phase of 10–15 min, representing less than 10 half-lives (Table

II), steady-state histone acetylation levels are only just beginning to rise. However, a dramatic increase by at least a factor of 3 is seen in acetate incorporation into histone H4 (Fig. 6D) and H3 (Fig. 6H), which both become labeled to a similar specific radioactivity. Even histone H2B becomes stronger labeled, reaching 0.3% of the specific radioactivity of H4 and the steady-state acetylation level may increase from 0.007 to 0.010 acetyl-lysines per molecule (results not shown). At much higher levels, H4 and H3 acetylation levels approximately double, as before (Fig. 5, C and F). It has been deduced that histone hyperacetylation will make chromatin less compact and more accessible to enzymes like DNase I and acetyltransferases (2, 45). However, the changes seen here are much too small to explain the strong increase in label incorporation. Most likely, TSA treatment affects labeling of the acetyl-CoA pool. Thus, the changes seen in tracer incorporation may not quantitatively reflect the extent to which histone deacetylases are inhibited by TSA *in vivo*. Despite this caveat, it is clear that the rate of histone acetylation slows down dramatically during the initial 40 min of TSA treatment; the rising slopes in hyperacetylating H4 and H3 forms flatten out (Fig. 6, C and G), and levels of tracer incorporation decrease, with apparent exponential half-lives of  $12 \pm 2$  min for histone H4 and  $9 \pm 1$  min for histone H3. This analysis revealed some additional differences in dynamic acetylation of these histones. Acetate incorporation into histone H3 became negligible by 90 min (Fig. 6H) when the hyperacetylation rate of H3 decreased to 0.1 acetyl-lysine addition per h per molecule (Fig. 6G). Tracer incorporation for histone H4 decreased to 40% (Fig. 6D), the same level as observed for H2B (results not shown), with a hyperacetylation rate of 0.4 acetyl-lysine addition per h per H4 after 90 min treatment with TSA (Fig. 6C). This rate apparently slows down further as no additional increase in H4 acetylation was detected between 7 and 25 h of culture with TSA (results not shown).

The pattern of tracer incorporation into acetylated forms of histone H4 (Fig. 6B) and H3 (Fig. 6F) confirms the conclusions

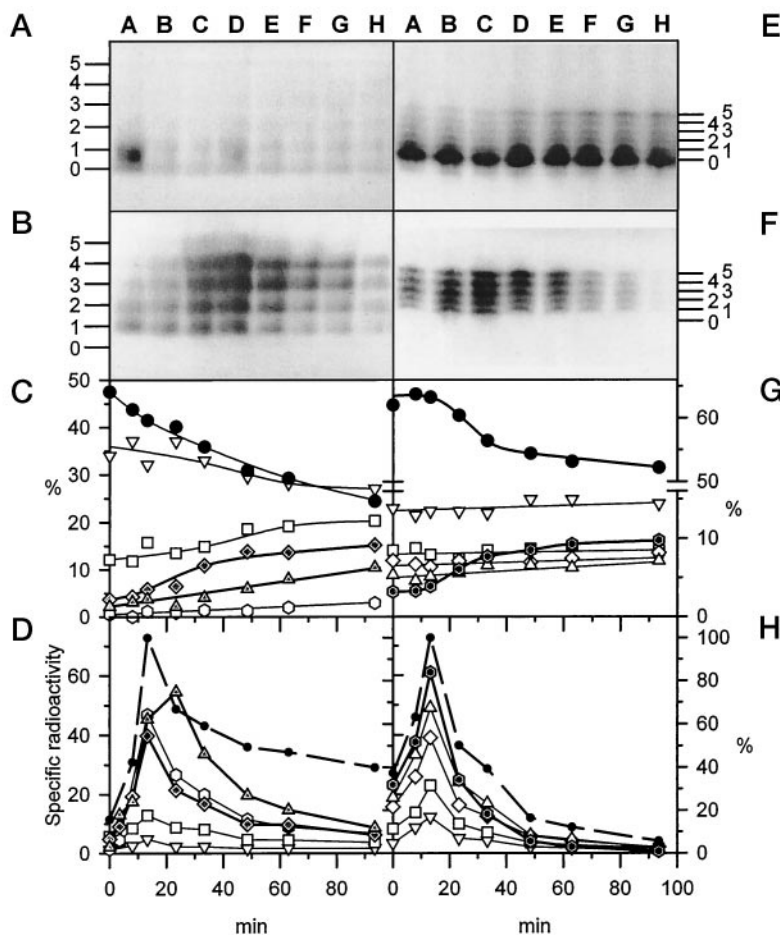


FIG. 6. TSA inhibition of histone deacetylase activity assessed *in vivo* by acetate tracer study. *Chlamydomonas* culture was made 10  $\mu\text{g/ml}$  cycloheximide, and after 10 min TSA was added to 100 ng/ml. Tritiated acetate (1 mCi, 10  $\mu\text{M}$ ) was added immediately (lane A) or after 5 (lane B), 10 (lane C), 20 (lane D), 30 (lane E), 45 (lane F), 60 (lane G), or 90 min (lane H). Cells were collected after 3 min and histones prepared. HPLC fractionated histone H4 (A) and H3 (E) were run on AUT gels, stained with Coomassie (A and E), densitometrically analyzed (C and G), fluorographed (B and F), and fluorograph exposures within a linear response window were quantitated (D and H). B shows a fluorograph of the histone H4 gel of A, exposed for 22 days. F shows a 2-day fluorograph of the histone H3 gel of E. The acetylation levels between 0 and 5 are indicated along A, B, E, and F. The symbols used in C, D, G, and H were for the following levels of acetylation: 0, solid circle; 1, inverted triangle; 2, square; 3, diamond; 4, triangle; 5, hexagon. Symbols were shaded for levels that showed the most significant pattern. The fraction of each acetylation level of Coomassie-stained H4 (left axis) is shown in C and of H3 (right axis) in G. The specific radioactivity, determined from the relative density of fluorograph and Coomassie stain, in arbitrary units, is given on the left axis of D and H plotted with continuous lines for distinct acetylation levels of histone H4 and histone H3, respectively. Along the right axis of both panels a relative scale is given for the total label incorporated in all forms of histone H4 (D) and histone H3 (H), marked by a broken line, setting to 100% the incorporation level achieved between 10 and 13 min treatment with TSA.

of relative turnover rates and dynamic site usage reached by acetate labeling studies in the absence of TSA. Although the absolute levels of label incorporation in histone H3 changes with time, the relative intensity of all bands stays approximately equal (Fig. 6F), roughly in proportion to the acetylation level between 1 and 5 (Fig. 6H). This is consistent with an equal but slowing rate of acetate label incorporation and turnover at every site in acetylated histone H3 molecules. In contrast, the faster turnover of acetylation in higher acetylated forms of histone H4 upon TSA treatment (Fig. 3B) results in a gradual shift with tracer incorporation into more highly acetylated forms (Fig. 6B) because only at these levels will residual deacetylase activity (Fig. 6D) create deacetylated lysines that can incorporate the acetate tracer during the last minutes of incubation.

#### DISCUSSION

Histone acetylation is a dynamic process that involves a significant fraction of the cellular chromatin, with high acetylation levels within transcribed chromatin domains and within

gene and whole DNA loop domains that are potentiated for transcription (14, 45). In plants, the fraction of the genome involved in dynamic acetylation displayed a clear correlation with the size of the genome (36), being higher in plants with smaller genomes where the fraction of transcribed chromatin is higher. *Chlamydomonas* may represent an extreme example. It has quite a small, haploid genome ( $10^9$  base pairs, 0.1 pg of DNA). Assuming that nucleosomes with dynamically, multi-acetylated histone H3 also contain dynamically acetylated H4, an assumption generally made and generically supported by a wide variety of experimental analyses, approximately 20% of the chromatin of *Chlamydomonas* is dynamically multi-acetylated with a half-life of approximately 2 min, the highest value reported to date. Nucleosomes in this chromatin would contain 10 or more acetylated lysines as follows: 3.2 acetyl-lysines on each of the two H3 histones, 1.6 dynamic and likely 0.2 non-dynamic acetyl-lysines on each of two H4 molecules and possibly pairs of H2B and H2A histones, each with less than 0.1 acetylated lysines. A similar level for total core histone acety-

lation, with predominant H3 acetylation, had been deduced for nucleosomes within destabilized, transcriptionally active chromatin of alfalfa (37).

The amino termini of histone H3 and H4 have been identified, together with linker histone H1, as a major force that stabilizes the condensed and repressed chromatin fiber (46–48). The recent x-ray analysis of the nucleosome at 2.8-Å resolution (49) allows one to localize a large part of these tails and speculate on the interactions that are changed upon lysine acetylation. The positively charged lysines in the H4 tails that exit from the sides of the histone octamer wedge would be reduced by nearly half in highly acetylated nucleosomes of *Chlamydomonas*, reducing or abolishing the detected side-by-side interactions with closely packed nucleosomes (34). The amino-terminal tail of histone H3 exits in the plane of the nucleosome between the DNA gyres (49), close to one of the linker histone H1-binding sites (50, 51), and is well known to cross-link with linker DNA and linker histone (52, 53). Loss of more than half of its lysine charges likely will cause loss of folding constraints on the chromatin fiber (54), a step toward release of linker histone and chromatin transcription (52). The preponderance of histone H3 multi-acetylation in dynamically acetylated chromatin in *Chlamydomonas* and higher plants (35, 36, 38, 39) suggests that constraining linker DNA may be more important to compact the inactive chromatin fiber in this group of organisms.

This paper demonstrates for the first time for green algae that TSA, as expected from *in vitro* inhibition of plant histone deacetylases (27), induces hyperacetylation of core histones. The simple deacetylase inhibitor *n*-butyrate may be ineffective during phototrophic growth because it is rapidly metabolized as in plant cells (38). TSA appears to be stable in *Chlamydomonas*, as judged by effective maintenance of hyperacetylated histones for at least 25 h (Fig. 5). Long term treatment of animal cells with butyrate, TSA, and other deacetylase inhibitors leads to a complete shift from predominantly non-acetylated histone H4 to largely multi-acetylated forms (2, 33, 55, 56). Thus, frequently, even more than 90% of histone H4 becomes acetylated, resulting from (slow) histone acetyltransferase action on nucleosomes in inactive chromatin. Histone H3 typically responds less completely (56). In a previous study, it had been noted that the relative distribution of non- through penta-acetylated histone H3 forms suggested that the difference in accessibility for acetylating enzymes between chromatin with non-acetylated and chromatin with acetylated histone H3 forms apparently was much larger than deduced for animal cells (39). The data collected in Table II confirmed this conclusion in the sense that apparently all acetylated H3 molecules and half of all acetylated histone H4 molecules are subject to continuous, rapid turnover of acetylation groups. TSA confirmed the complementary part of the conclusion by showing that even after 24 h only 20% of non-acetylated H3 became acetylated (Fig. 5E) and that a similar limited decrease occurred for histone H4 (Fig. 5B). Thus, the structure of nucleosomes and chromatin fibers of *Chlamydomonas*, derived from the abundant 20% fraction that is dynamically multi-acetylated at H3 and H4 with 10 or more acetylated lysines, should be compared with the chromatin structure, 50% of total, that remains unacetylated even after 24 h treatment with TSA. Such a study may recognize new differences between transcriptionally repressed and activated chromatin that are present in a less pronounced fashion in the chromatin of higher eukaryotes.

**Acknowledgments**—I gratefully acknowledge the research opportunities created by Dr. M. Martinez-Carrion, fruitful discussions with Dr. T. Kapros, and the use of the CO<sub>2</sub> air compressor of Dr. M. Schaefer.

## REFERENCES

- Allfrey, V. G. (1977) in *Chromatin and Chromosome Structure* (Li, H. J., and Eckhardt, R. A., eds) pp. 167–191, Academic Press, New York
- Matthews, H. R., and Waterborg, J. H. (1985) in *The Enzymology of Post-translational Modification of Proteins* (Freedman, R. B., and Hawkins, H. C., eds) Vol. 2, pp. 125–285, Academic Press, London
- Sealy, L., and Chalkley, R. (1978) *Cell* **14**, 115–121
- Jackson, V., Shires, A., Chalkley, R., and Granner, D. K. (1975) *J. Biol. Chem.* **250**, 4856–4863
- Covault, J., and Chalkley, R. (1980) *J. Biol. Chem.* **255**, 9110–9116
- Zhang, D. E., and Nelson, D. A. (1988) *Biochem. J.* **250**, 233–240
- Waterborg, J. H., and Matthews, H. R. (1983) *Biochemistry* **22**, 1489–1496
- Davie, J. R., and Hendzel, M. J. (1994) *J. Cell. Biochem.* **55**, 98–105
- Nelson, D. A., and Alonso, W. R. (1983) *Biochim. Biophys. Acta* **741**, 269–271
- Nelson, D. A. (1982) *J. Biol. Chem.* **257**, 1565–1568
- Turner, B. M., Birley, A. J., and Lavender, J. (1992) *Cell* **69**, 375–384
- Lin, R., Leone, J. W., Cook, R. G., and Allis, C. D. (1989) *J. Cell Biol.* **108**, 1577–1588
- Braunstein, M., Sobel, R. E., Allis, C. D., Turner, B. M., and Broach, J. R. (1996) *Mol. Cell Biol.* **16**, 4349–4356
- Hebbes, T. R., Thorne, A. W., and Crane-Robinson, C. (1988) *EMBO J.* **7**, 1395–1402
- Grunstein, M. (1997) *Nature* **389**, 349–352
- Zhang, D. E., and Nelson, D. A. (1988) *Biochem. J.* **250**, 241–246
- Yoshida, M., Horinouchi, S., and Beppu, T. (1995) *BioEssays* **17**, 423–430
- Kwon, H. J., Owa, T., Hassig, C. A., Shimada, J., and Schreiber, S. L. (1998) *Proc. Natl. Acad. Sci. U. S. A.* **95**, 3356–3361
- Darkin-Rattray, S. J., Gurnett, A. M., Myers, R. W., Dulski, P. M., Crumley, T. M., Allocco, J. J., Cannova, C., Meinke, P. T., Colletti, S. L., Bednarek, M. A., Singh, S. B., Goetz, M. A., Dombrowski, A. W., Polishook, J. D., and Schmatz, D. M. (1996) *Proc. Natl. Acad. Sci. U. S. A.* **93**, 13143–13147
- Brownell, J. E., Zhou, J. X., Ranalli, T., Kobayashi, R., Edmondson, D. G., Roth, S. Y., and Allis, C. D. (1996) *Cell* **84**, 843–851
- Kadonaga, J. T. (1998) *Cell* **92**, 307–314
- Mizzen, C. A., and Allis, C. D. (1998) *Cell. Mol. Life Sci.* **54**, 6–20
- Hassig, C. A., Tong, J. K., Fleischer, T. C., Owa, T., Grable, P. G., Ayer, D. E., and Schreiber, S. L. (1998) *Proc. Natl. Acad. Sci. U. S. A.* **95**, 3519–3524
- Wolffe, A. P. (1997) *Nature* **387**, 16–17
- Lopez-Rodas, G., Georgieva, E. I., Sendra, R., and Loidl, P. (1991) *J. Biol. Chem.* **266**, 18745–18750
- Lusser, A., Brosch, G., Loidl, A., Haas, H., and Loidl, P. (1997) *Science* **277**, 88–91
- Lechner, T., Lusser, A., Brosch, G., Eberharder, A., Goralik-Schramel, M., and Loidl, P. (1996) *Biochim. Biophys. Acta* **1296**, 181–188
- Sendra, R., Rodrigo, I., Salvador, M. L., and Franco, L. (1988) *Plant Mol. Biol.* **11**, 857–868
- Rundlett, S. E., Carmen, A. A., Kobayashi, R., Bavykin, S., Turner, B. M., and Grunstein, M. (1996) *Proc. Natl. Acad. Sci. U. S. A.* **93**, 14503–14508
- Kuo, M.-H., Brownell, J. E., Sobel, R. E., Ranalli, T. A., Cook, R. G., Edmondson, D. G., Roth, S. Y., and Allis, C. D. (1996) *Nature* **383**, 269–272
- Wade, P. A., Pruss, D., and Wolffe, A. P. (1997) *Trends Biochem. Sci.* **22**, 128–131
- Struhl, K. (1998) *Genes Dev.* **12**, 599–606
- Almouzni, G., Khochin, S., Dimitrov, S., and Wolffe, A. P. (1994) *Dev. Biol.* **165**, 654–669
- Rundlett, S. E., Carmen, A. A., Suka, N., Turner, B. M. A., and Grunstein, M. (1998) *Nature* **392**, 831–835
- Waterborg, J. H. (1991) *Plant Physiol. (Bethesda)* **96**, 453–458
- Waterborg, J. H. (1992) *Plant Mol. Biol.* **18**, 181–187
- Waterborg, J. H. (1993) *J. Biol. Chem.* **268**, 4912–4917
- Waterborg, J. H., Harrington, R. E., and Winicov, I. (1990) *Biochim. Biophys. Acta* **1049**, 324–330
- Waterborg, J. H., Robertson, A. J., Tatar, D. L., Borza, C. M., and Davie, J. R. (1995) *Plant Physiol. (Bethesda)* **109**, 393–407
- Waterborg, J. H. (1990) *J. Biol. Chem.* **265**, 17157–17161
- Belyaev, N. D., Houben, A., Baranczewski, P., and Schubert, I. (1997) *Chromosoma* **106**, 193–198
- Fabry, S., Müller, K., Lindauer, A., Park, P. B., Cornelius, T., and Schmitt, R. (1995) *Curr. Genet.* **28**, 333–345
- Walther, Z., and Hall, J. L. (1995) *Nucleic Acids Res.* **23**, 3756–3763
- Waterborg, J. H. (1992) *Biochemistry* **31**, 6211–6219
- Hebbes, T. R., Clayton, A. L., Thorne, A. W., and Crane-Robinson, C. (1994) *EMBO J.* **13**, 1823–1830
- Thomas, J. O. (1984) *J. Cell Sci.* **1**, (suppl.) 1–20
- Allan, J., Harborne, N., Rau, D. C., and Gould, H. (1982) *J. Cell Biol.* **93**, 285–297
- Allan, J., Mitchell, T., Harborne, N., Bohm, L., and Crane-Robinson, C. (1986) *J. Mol. Biol.* **187**, 591–602
- Luger, K., Mäder, A. W., Richmond, R. K., Sargent, D. F., and Richmond, T. J. (1997) *Nature* **389**, 251–260
- Pruss, D., Bartholomew, B., Persinger, J., Hayes, J., Arents, G., Moudrianakis, E. N., and Wolffe, A. P. (1996) *Science* **274**, 614–617
- Hayes, J. J. (1996) *Biochemistry* **35**, 11931–11937
- Van Holde, K. E. (1989) *Chromatin*, Springer-Verlag Inc., New York
- Kurochikina, L. P., and Kolomijtseva, G. Y. (1992) *Biochem. Biophys. Res. Commun.* **187**, 261–267
- An, W. J., Leuba, S. H., Van Holde, K., and Zlatanova, J. (1998) *Proc. Natl. Acad. Sci. U. S. A.* **95**, 3396–3401
- Marvin, K. W., Yau, P., and Bradbury, E. M. (1990) *J. Biol. Chem.* **265**, 19839–19847
- Pantazis, P., and Bonner, W. M. (1982) *J. Cell. Biochem.* **20**, 225–235